A CisplatinLoaded Immunochemotherapeutic Nanohybrid Bearing Immune Checkpoint Inhibitors for Enhanced Cervical Cancer Therapy

Angewandte
GDCh
Eine Zeitschrift der Gesellschaft Deutscher Chemiker
Chemie
www.angewandte.de

Akzeptierter Artikel

Titel: A cisplatin-loaded immuno-chemotherapeutic nanohybrid bearing immune checkpoint inhibitors for enhanced cervical cancer therapy

Autoren: Na Wang, Zhigang Wang, Zoufeng Xu, Xianfeng Chen, and Guangyu Zhu

Zitierweise: *Angew. Chem. Int. Ed.* 10.1002/anie.201800422
Angew. Chem. 10.1002/ange.201800422

Link zur VoR: http://dx.doi.org/10.1002/anie.201800422
http://dx.doi.org/10.1002/ange.201800422

WILEY-VCH

10.1002/ange.201800422

WILEY-VCH

COMMUNICATION

A Cisplatin-Loaded Immuno-Chemotherapeutic Nanohybrid Bearing Immune Checkpoint Inhibitors for Enhanced Cervical Cancer Therapy

Na Wang, Zhigang Wang, Zoufeng Xu, Xianfeng Chen, and Guangyu Zhu*

Abstract: *The efficacy of conventional chemotherapy is hindered by cancer cells' escape from the immune system. Herein, we report a multifunctional nanohybrid system for effective immuno-chemotherapy against cervical cancer. This nanohybrid contains both immune checkpoint inhibitor and cisplatin anticancer prodrug, showing improved cellular accumulation and increased binding of Pt to DNA and resulting in elevated apoptosis than using cisplatin alone when tested in cervical cancer cells. Intriguingly, the use of immune checkpoint inhibitors enables the inhibition of indoleamine-2,3-dioxygenase and reverses immunosuppressive T cells to recognize cancer cells, leading to T cell proliferation and activation, cancer cell cycle arrest, and ultimately increased cancer cell death. The nanohybrid is also active in vivo against the growth of human cervical tumor. Overall, we provide a novel strategy using a multifunctional nanohybrid system to boost the antitumor activity of cisplatin, the gold standard chemotherapeutic treatment for cervical cancer.*

Immune response against cancer is developed by innate effector cells and particularly relies on T cells,[1] which are sensitive to the level of tryptophan.[2] In the presence of cancer cells, tryptophan is degraded to kynurenine by indoleamine-2,3-dioxygenase (IDO), an essential enzyme in the kynurenine pathway.[3] The tryptophan metabolites or inadequate tryptophan consequently lead to T cell anergy, tilting the immune system toward tumor support.[4] Recently, small molecules have emerged to address IDO inhibition and revive T cells for cancer immunotherapy.[5] The front-runner of IDO inhibitors, D-1-methyl-tryptophan (D-1MT), has entered clinical trials against multiple types of cancers,[6] but the detailed mechanism of this weak IDO inhibitor is still controversial.[7] More specific and potent IDO inhibitors are in the pipeline.[8] Although IDO inhibitors as well as other immune checkpoint inhibitors have launched inspired clinical successes for cancer immunotherapy, satisfactory tumor regression has been only achieved in some patients with advanced cancer, while other patients do not respond, indicating a large room to further improve.[9]

Some common chemotherapies are potentiated by IDO inhibitors.[10] For example, cisplatin, a first-line chemotherapeutic in clinics,[11] can induce more significant tumor regressions than single-agent therapy when combined with IDO inhibitors.[10] Besides, with the addition of cisplatin, the T cell-mediated antitumor immunity is enhanced by indirectly producing additional proinflammatory signals.[10, 12] Thus, a combination of cisplatin with IDO inhibitors may strengthen the dual advantages and overcome the limitations of immunotherapy and chemotherapy. Delivery of cisplatin together with IDO inhibitors will take advantage of not only the potential synergism from the two warheads but also delivery vehicles to achieve enhanced anticancer efficacy; however, the development of such an effective anticancer complex is still a nascent area.

Herein, we report an immuno-chemotherapeutic weapon for enhanced cervical cancer therapy. A nanohybrid ratiometrically co-loaded with IDO inhibitor and cisplatin prodrug was assembled, expected to be effective against cancer cells by killing them with cisplatin but simultaneously stimulating T cells to promote the apoptosis of cancer cells. This strategy of treating cervical cancer with immuno-chemotherapeutic nanomedicine to stimulate the function of T cells through IDO blocking might provide a new way of conquering cervical tumor especially that responds poorly to conventional chemotherapeutics.

To assemble a nanohybrid co-loaded with IDO inhibitors and chemotherapeutics, a reliable nanoparticle system is required. Layered double hydroxide (LDH) nanoparticles were utilized in our study, as they are biocompatible and biodegradable, with low toxicity and high cancer-cell selectivity.[13] We choose 4-{[2-(4-bromophenyl)hydrazinyl]sulfonyl}benzoic acid, a more potent IDO inhibitor (IDOi) than D-1MT, as the immune checkpoint inhibitor.[14] For chemotherapeutic regimen, a cisplatin prodrug *c,c,t*-[$Pt(NH_3)_2Cl_2(O_2CCH_2CH_2COOH)_2$] (disuccinatocisplatin, DSCP) is utilized. In our design, the anionic property of both IDOi and the cisplatin prodrug ensures their efficient co-loading into the interlayer regions of LDH nanoparticles through anion exchange. More importantly, we take advantage of Pt(IV) prodrugs including lowered toxicity and efficient activation by intracellular reductants.[15] We expect that the nanohybrid enters cells through endocytotic pathways and the Pt(IV) prodrug is released from the nanohybrid and induces apoptosis in cancer cells; simultaneously, the IDOi discharges from the nanohybrid and boosts the T cell proliferation and immune response against cancer cells in a tumor microenvironment (Scheme 1).

Mg/Al LDH nanoparticles were fabricated through our previously established method.[16] Various ratios of DSCP and IDOi were subsequently co-loaded into LDH nanoparticles by anion exchange, and the loaded nanohybrid was designated as

* N. Wang, Dr. Z. Wang, Z. Xu, Prof. Dr. G. Zhu
Department of Chemistry
City University of Hong Kong
83 Tat Chee Ave, Kowloon Tong, Hong Kong SAR (P. R. China)
E-mail: guangzhu@cityu.edu.hk

Prof. Dr. X. Chen
Institute for Bioengineering, School of Engineering
The University of Edinburgh
King's Buildings, Mayfield Road, Edinburgh EH9 3JL, UK

N. Wang, Dr. Z. Wang, Z. Xu, Prof. Dr. G. Zhu
City University of Hong Kong Shenzhen Research Institute,
Shenzhen (P. R. China)

Supporting information for this article is given via a link at the end of the document.

10.1002/ange.201800422

Pt(IV)-IDOi/LDH. Pt contents in the nanohybrid were measured by inductively coupled plasma-optical emission spectroscopy (ICP-OES), while the concentration of IDOi was determined by UV-vis spectroscopy. The molar ratios of the loaded Pt to IDOi in LDH were determined to be 10:1, 1:2, 1:10, 1:40, and 1:245. Pt(IV)/LDH and IDOi/LDH were assembled as controls (Table S1).

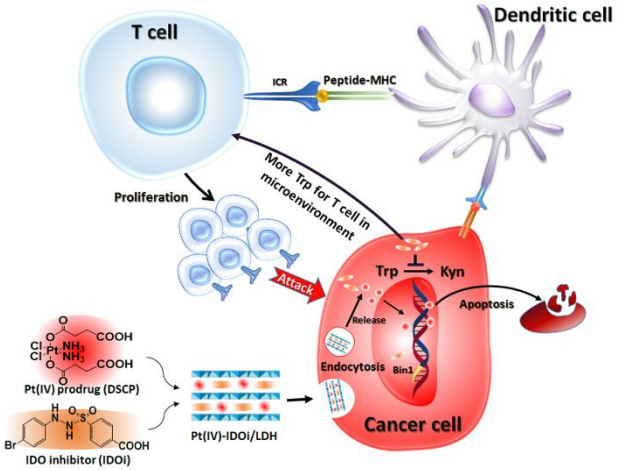

Scheme 1. Strategic overview of a cisplatin-loaded nanohybrid for immuno-chemotherapy. The nanohybrid Pt(IV)-IDOi/LDH enters cancer cells and releases Pt(IV) prodrug and IDOi. The former is reduced to cisplatin that binds to genomic DNA to induce cancer cell apoptosis; simultaneously, the latter blocks the pathway to produce kynurenine, leaving more tryptophan in the microenvironment for T cell proliferation and development. With the checkpoint inhibitor IDOi, proliferated T cells can distinguish cancer cell through the signal from antigen present cell (APC, such as dendritic cell), and enhance the chemotherapy. At last, the nanohybrid elevates cancer cell cycle arrest and apoptosis. Abbreviations are as follows: IDO, indoleamine-2,3-dioxygenase; TCR, T cell receptor; MHC, major histocompatibility complex; Trp, tryptophan; Kyn, kynurenine.

The nanohybrid was characterized by transmission electron microscopy (TEM) and dynamic light scattering (DLS) measurement. The TEM images illustrate the typical hexagonal morphology of LDH, Pt(IV)/LDH, and IDOi/LDH (Figure S1). Apparently, for Pt(IV)-IDOi/LDH with different co-loading ratios (10:1, 1:2, 1:10, and 1:40), the nanohybrid remains the typical morphology of LDH. However, when the ratio of Pt(IV) to IDOi reaches 1:245, the nanohybrid aggregates and forms several clusters (Figure S1). Therefore, the Pt(IV)-IDOi/LDH with the loading ratio of 1:245 was excluded from further investigation. With the successful insertion of Pt(IV) and IDOi into LDH nanoparticles, the decrease of zeta potential and the increase of hydrodynamic size are noted (Table S2). The gradual decrease of zeta potential is ascribed to the increased loading amount of negatively charged DSCP and IDOi, neutralizing the positively charged LDH. The average hydrodynamic size of LDH is 73.8 ± 2.1 nm, and the value steadily increases to 117.2 ± 5.1, 158.2 ± 18.9, 176.9 ± 11.6, and 216.7 ± 30.8 nm for Pt(IV)-IDOi/LDH with Pt(IV):IDOi ratios of 10:1, 1:2, 1:10, and 1:40, respectively (Table S2).

The cytotoxicities of the nanohybrid against HeLa and A549 cancer cells were determined. HCvEpC human cervical epithelial cells and WI-38 human lung fibroblast cells were included as comparisons (Table 1). HeLa and A549 cells were chosen because the expression levels of IDO are higher in those cells especially the former than others including MCF-7, A2780, and A549cisR (Figure S2). LDH nanoparticles themselves show negligible cytotoxicity with IC_{50} > 400 μg/mL in the two cell lines. Cisplatin shows typical IC_{50} values in the low micromolar range. Pt(IV)/LDH has a higher cytotoxicity than cisplatin, indicating the efficiency of the delivery system. The IC_{50} values of Pt(IV)-IDOi/LDH with a loading ratio of 1:2, 1:10, and 1:40 in HeLa cells are 1.5 ± 0.3, 0.7 ± 0.5, and 0.3 ± 0.1 μM, respectively. Clearly, Pt(IV)-IDOi/LDH exhibits more significant cytotoxicity in the cervical cancer cells. Moreover, the increased amount of IDOi enhances the cytotoxicity of the nanohybrid, which is likely from the inhibition of tryptophan degradation.[17] A similar trend is observed in A549 cells, and the Pt(IV)-IDOi(1:40)/LDH shows the highest cytotoxicity in the sub-micromolar range. In contrast, the nanohybrid is not significantly active in IDO-expressing HCvEpC and WI-38 cells (Figure S2). The cytotoxicity of Pt(IV)-IDOi(1:40)/LDH toward HCvEpC cells is 26-time lower than that in HeLa cells, while the cytotoxicity in WI-38 cells shows 16-time lower than that in A549 cells, suggesting the high cancer-cell selectivity of the nanohybrid. Since Pt(IV)-IDOi(1:40)/LDH shows the highest cytotoxicity in the IDO-expressing HeLa cells, we utilize this sample and the cervical cancer cells for the following biological assays.

Cancer cells can be disguised by kynurenine and are able to evade from the immune system via IDO-mediated tryptophan pathway.[18] Hence, the capacity of Pt(IV)-IDOi(1:40)/LDH to block kynurenine production in HeLa cells was examined. An Ehrlich's reagent (2% *p*-dimethylaminobenzaldehyde) was utilized to react with kynurenine, and the level of this tryptophan metabolite was quantified.[19] The half maximum effect concentration (EC_{50}) shown in Table S3 and the level of kynurenine in Figure S5 represent the inhibitory efficacy of kynurenine production in HeLa cells. D-1MT has an EC_{50} value of >1 mM, confirming its weak inhibitory effect. The IDOi we use shows a stronger inhibitory effect than D-1MT against the catalytic activity of IDO in HeLa cells with an EC_{50} value of 163 ± 24 μM. In contrast, IDOi/LDH is very effective in blocking the kynurenine production, and its EC_{50} value is 4.0 ± 0.3 μM, indicating the efficient delivery of IDOi into the cells. Intriguingly, Pt(IV)-IDOi(1:40)/LDH shows the highest activity with an EC_{50} value of 1.9 ± 0.2 μM against kynurenine

Table 1. Cytotoxicity of different complexes in HeLa, A549, and WI-38 cells. The cells were incubated with complexes for 72 h, and cell viability was tested by MTT assay.

Complex	IC_{50}/μM[a]			
	HeLa	A549	HCvEpC	WI-38
LDH[b]	> 400	> 400	N.D.	N.D.
Cisplatin	5.1 ± 2.0	2.6 ± 0.6	1.4 ± 0.4	3.3 ± 1.4
Pt(IV)/LDH	3.5 ± 1.0	N.D.[c]	8.9 ± 2.3	17.2 ± 6.8
IDOi/LDH	9.1 ± 4.3	N.D.	N.D.	N.D.
Pt(IV)-IDOi(10:1)/LDH	4.7 ± 2.0	N.D.	N.D.	N.D.
Pt(IV)-IDOi(1:2)/LDH	1.5 ± 1.0	5.0 ± 0.6	N.D.	N.D.
Pt(IV)-IDOi(1:10)/LDH	0.7 ± 0.5	1.5 ± 0.3	N.D.	N.D.
Pt(IV)-IDOi(1:40)/LDH	0.3 ± 0.1	0.7 ± 0.2	7.9 ± 2.9	11.1 ± 2.7
D-1MT	7900 ± 261	> 1000	N.D.	N.D.

[a] For complexes containing Pt, the concentration equivalent to Pt concentration. [b] The unit of LDH is presented as μg/mL. [c] N.D. Not determined.

10.1002/ange.201800422

production, showing the effectiveness of the nanohybrid to inhibit IDO.

With the reduction of kynurenine production, T cells can proliferate to boost anti-tumor immune responses.[20] Mixed leukocyte reactions (MLRs) is applied for measuring the cellular immune response in vitro. Human peripheral blood mononuclear cells (PBMCs) were employed to mimic the immune microenvironment in the body because it consists of lymphocytes and monocytes.[21] A double-staining flow cytometric assay was applied for the detection of T cell proliferation. In the experiment, PBMCs from unrelated healthy donors were stimulated by phytohemagglutinin-M (PHA-M), a lectin, for T cell activation. The cells were subsequently stained with carboxyfluorescein succinimidyl ester (CFSE), a fluorescent cell staining dye without adverse effect to cell health, and co-cultured with adherent HeLa cells. The HeLa/MLRs were treated with the complexes, and PBMCs were harvested and stained with a FITC-conjugated anti-CD3 antibody. Here, CD3 acts as a marker representing the development of T cells, which is also required for T cell activation.[22] After treatment, CFSE-labeled and $CD3^+$ dual-positive T cells were analyzed for the changes of proliferating T cells. The depleting of IDO enzyme induced by our nanohybrid may lead to T cell proliferation in this HeLa/MLRs system.

When HeLa cells are mixed with PBMCs without any treatment, the percentage of T cell proliferation is as low as 5.6% (Figure 1A). In the group containing a mixture of D-1MT and cisplatin, 29.8% of T cells proliferate, and the value increases to 35.3% for a mixture of IDOi and cisplatin, indicating the effectiveness of IDOi in stimulating T cell activity (Figure 1B and 1C). Remarkably, HeLa/MLRs treated with Pt(IV)-IDOi(1:40)/LDH have 41.9% of T cell proliferation, which is higher than the results from the control or the co-treatment without nanocarrier, showing that our nanohybrid can effectively stimulate the proliferation of T cells (Figure 1D). The subsequent generation of divided T cells was then analyzed based on the increasing dilution of CFSE. Each additional peak, shown in the pink color in Figure 1, indicates one subsequent generation of T cells. After 6 days, the HeLa/MLRs incubated with Pt(IV)-IDOi(1:40)/LDH apparently show more T cell generations than all the other groups, further confirming the proliferation of T cells. Together with the cytotoxicity results above, it is obvious that our nanohybrid is an effective immuno-chemotherapeutic agent that can simultaneously kill cervical cancer cells and stimulate T cell proliferation.

The above-mentioned HeLa/MLRs system only corroborates the proliferation of T cells, but the subsequent effect on cancer cells is still unknown. To know this, cell cycle distribution of HeLa cells in the presence of PBMCs after treatment with Pt(IV)-IDOi/LDH was measured. HeLa cells without treatment display a normal profile of cell cycle distribution (Figure 2A). The cells treated with Pt(IV)-IDOi/LDH without the presence of PBMCs are arrested at the S phase (43.2%), and we attribute this cell cycle arrest to the efficient delivery of cisplatin prodrug into HeLa cells to arrest the cell cycle. In contrast, our nanohybrid arrests the HeLa cells at the S phase more strongly in the presence of PBMCs. Under this condition, 67.6% of the cells stay at the S phase, indicating the role of activated T cells in arresting the cell cycle of HeLa cells, possibly through the blockage of Cytotoxic T-Lymphocyte Antigen 4 (CTLA-4) ligands.[23]

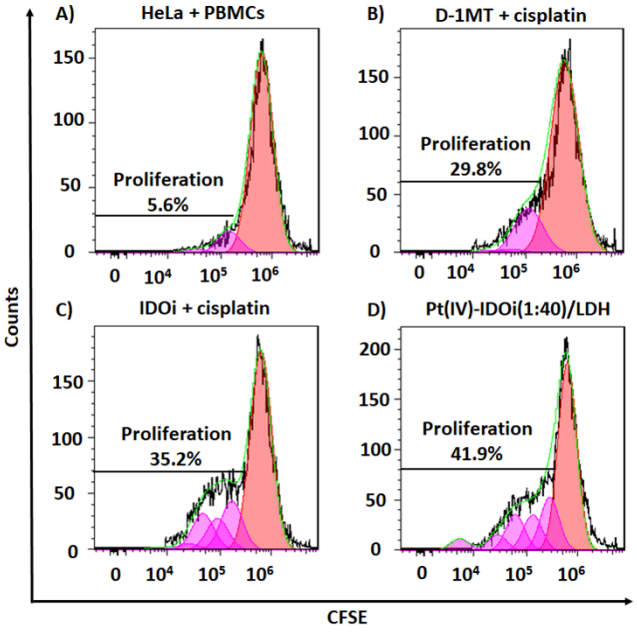

Figure 1. Measurement of T cell proliferation in HeLa/MLRs system after cultured with/without different complexes for 6 days. A) medium only, B) 1.6 μM D-1MT and 0.04 μM cisplatin, C) 1.6 μM IDOi and 0.04 μM cisplatin, and D) Pt(IV)-IDOi(1:40)/LDH (equivalent to 1.6 μM IDOi and 0.04 μM Pt) were added in the HeLa/MLRs co-culture system. After 6 days, the CFSE-labeled CD3+ T cells were quantified using a flow cytometer. Black line – population signal of dual-positive stained cells detected from flow cytometry; green line – fitting curves of black line for T cell proliferation analysis. Each additional peak (pink) indicates one subsequent generation of T cells analysed by software. The details are given in the Supplementary Information.

The apoptotic level of HeLa cells after T cell proliferation and activation in the HeLa/MLRs co-culture system was further examined. HeLa or HeLa/MLRs cells were exposed to Pt(IV)-IDOi/LDH, and HeLa cells were subsequently harvested and stained with Annexin V-FITC/7-AAD for flow cytometric analysis. For untreated group, the fractions of early apoptotic and late apoptotic cells are 2.6% and 14.1%, respectively (Figure 2B). In Pt(IV)-IDOi/LDH-treated group, the values significantly increase to 39.7% and 23.6% for early apoptosis and late apoptosis, respectively, indicating that our nanohybrid is able to effectively induce apoptosis in HeLa cells due to the presence of the chemotherapeutic warhead (Figure 2C). Particularly, when the cells were treated with the same concentration of the nanohybrid in the presence of PBMCs, significant escalation of late apoptosis (53.9%) was observed (Figure 2D). Apoptotic induction ability of the nanohybrid was further illustrated by labeling the fragmented DNA with the use of a TUNEL assay. Apoptosis occurred in HeLa cells treated with the nanohybrid in and without the presence of PBMCs (Figure S6). Apparently, the presence of PBMCs results in a higher level of apoptosis (50.2%) compared with the nanohybrid alone (33.9%) (Figure S7). Therefore, the presence of

10.1002/ange.201800422

activated T cells accelerates the apoptosis of the cervical cancer cells. Collectively, the data suggest that T cell activation is able to arrest the cell cycle and promote apoptosis in cancer cells when treated with our nanohybrid.

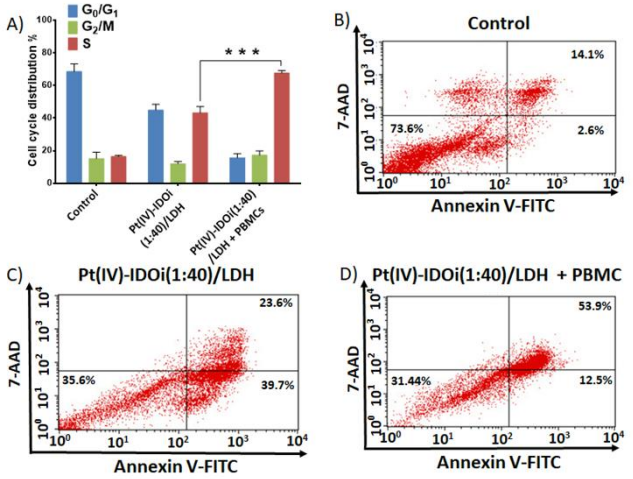

Figure 2. Flow cytometry analysis of A) cell cycle arrest of untreated cell and in complex with/ without PBMCs. Flow cytometry analysis of apoptosis with B) Annexin V/7-AAD staining of HeLa as control, C) Pt(IV)-IDOi(1:40)/LDH and D) Pt(IV)-IDOi(1:40)/LDH with PBMCs, after 3 days of culture. [Pt] = 5 μM. *** $p < 0.001$, Student's t-Test. Mean ± SD.

The antitumor activity of our nanohybrid *in vivo* was further demonstrated. Because BSA-coated LDH nanoparticles have shown great biocompatibility *in vivo*,[24] we prepared BSA-coated Pt(IV)-IDOi(1:40)/LDH. The shape, size, and zeta potential of the BSA-coated nanohybrid do not change significantly after 24 h incubation in blood plasma (Figures S11, S12, and Tables S4, S5). The BSA-coated nanohybrid was then used for an anticancer efficacy test in nude mice bearing HeLa xenograft. To verify the immuno-chemotherapeutic function of our nanohybrid, PHA-M-stimulated PBMCs were intravenously (*i.v.*) injected into two groups of mice to engraft human immune system in the immunodeficient mice after the HeLa tumor nodules were palpable.[25] Twenty four hours after PBMCs injection, BSA-coated Pt(IV)-IDOi(1:40)/LDH or PBS were injected (*i.v.*) for total 4 times at one day interval (Figures 3 and S13). After 14 days, BSA-coated Pt(IV)-IDOi(1:40)/LDH exhibits significantly stronger tumor inhibition than the other two groups ($p < 0.001$). Notably, the size of tumors in the group of PBMCs with the nanohybrid (291.7 ± 125.6 mm^3) is significantly smaller than the one in the group treated with the nanohybrid only (662.2 ± 168.5 mm^3) ($p < 0.05$), suggesting the effectiveness of our immuno-chemotherapeutic warhead in the presence of PBMCs. The body weight of each group increases gradually, indicating the safety of our nanohybrid (Figure S14). The level of free kynurenine and tryptophan in tumors was quantified by HPLC. Both the level of kynurenine and the ratio of kynurenine to tryptophan significantly decrease in the nanohybrid-treated groups compared with the untreated ones (Figure S15), revealing the inhibition of IDO by the nanohybrid *in vivo*. These results further confirm the efficacy of the nanohybrid in immune-chemotherapy *in vivo*.

In summary, we report the first example of a nanohybrid system bearing both IDOi and cisplatin as an immune-chemotherapeutic weapon to significantly boost the antitumor activity of cisplatin against cervical cancer. The nanohybrid containing chemotherapeutic regiments displays dramatically increased capability to kill HeLa cells without the presence of PBMCs, with a 17-fold increase in cytotoxicity compared with cisplatin alone. Remarkably, the presence of PBMCs in the system significantly boosts the antitumor activity of the nanohybrid, evidenced by the activation of T cells, the cell cycle arrest of HeLa cells induced by T cells, and the significantly increased fraction of late apoptotic HeLa cells resulted from the T cell activation. Compared with a small-molecule conjugate of D-1MT and cisplatin,[26] our nanohybrid apparently has many advantages, such as capability of tuning the ratio of IDOi and cisplatin to maximize the effectiveness of the system, limited premature reduction of cisplatin prodrug protected by nanoparticles,[27] cancer cell specificity, and potential passive tumor targeting due to the enhanced permeability and retention (EPR) effect. Our nanohybrid is, therefore, a very powerful antitumor complex utilizing a combinatorial strategy of both chemotherapy and immunotherapy, conveying a drug delivery system based on nanoparticles to overcome the current issues of efficient cancer therapy.

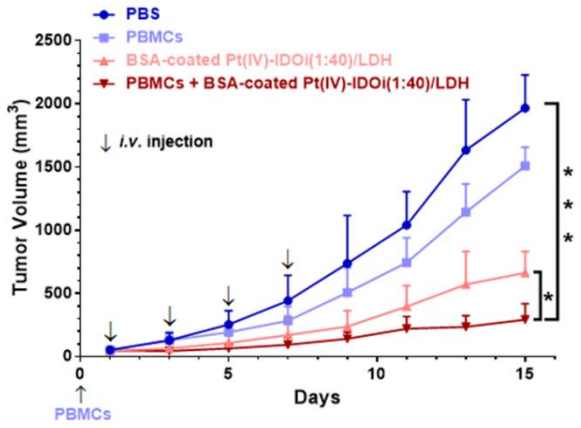

Figure 3. The growth of HeLa tumors in xenograft model with various treatment groups indicated. PBMCs (5 x 10^6 cells/mouse) were injected intravenously on Day 0. BSA-coated Pt(IV)-IDOi(1:40)/LDH ([Pt] = 0.5 mg/kg) was injected for total 4 times of injection. The tumor volume of each group was measured every two days for 14 days of duration. * $p < 0.05$, *** $p < 0.001$, Student's t-Test. Mean ± SD, n = 5.

Acknowledgements

We thank the National Natural Science Foundation of China (Grant No. 21371145) and the City University of Hong Kong (Projects 9667114, 9667131, and 9667148) for funding support.

Keywords: Immuno-chemotherapy • cisplatin • IDO inhibitor • Pt(IV) prodrug • cervical cancer

[1] a) I. Mellman, G. Coukos, G. Dranoff, *Nature* **2011**, *480*, 480-489; b) C. A. Klebanoff, S. A. Rosenberg, N. P. Restifo, *Nat. Med.* **2016**, *22*, 26-36.

[2] A. L. Mellor, D. H. Munn, *Nat. Rev. Immunol.* **2004**, *4*, 762-774.
[3] a) D. M. Pardoll, *Nat. Rev. Cancer* **2012**, *12*, 252-264; b) G. Frumento, R. Rotondo, M. Tonetti, G. Damonte, U. Benatti, G. B. Ferrara, *J. Exp. Med.* **2002**, *196*, 459-468.
[4] a) C. Uyttenhove, L. Pilotte, I. Theate, V. Stroobant, D. Colau, N. Parmentier, T. Boon, B. J. Van den Eynde, *Nat. Med.* **2003**, *9*, 1269-1274; b) R. Meisel, A. Zibert, M. Laryea, U. Göbel, W. Däubener, D. Dilloo, *Blood* **2004**, *103*, 4619-4621; c) D. H. Munn, A. L. Mellor, *J. Clin. Invest.* **2007**, *117*, 1147-1154.
[5] A. L. Mellor, D. B. Keskin, T. Johnson, P. Chandler, D. H. Munn, *J. Immunol.* **2002**, *168*, 3771-3776.
[6] S. Lob, A. Konigsrainer, H.-G. Rammensee, G. Opelz, P. Terness, *Nat. Rev. Cancer* **2009**, *9*, 445-452.
[7] a) A. J. Muller, P. A. Scherle, *Nat. Rev. Cancer* **2006**, *6*, 613-625; b) F. Qian, J. Villella, P. K. Wallace, P. Mhawech-Fauceglia, J. D. Tario, Jr., C. Andrews, J. Matsuzaki, D. Valmori, M. Ayyoub, P. J. Frederick, A. Beck, J. Liao, R. Cheney, K. Moysich, S. Lele, P. Shrikant, L. J. Old, K. Odunsi, *Cancer Res.* **2009**, *69*, 5498-5504; c) J. L. Adams, J. Smothers, R. Srinivasan, A. Hoos, *Nat. Rev. Drug Discov.* **2015**, *14*, 603-622.
[8] C. Sheridan, *Nat. Biotech.* **2015**, *33*, 321-322.
[9] a) J. Couzin-Frankel, *Science* **2013**, *342*, 1432-1433; b) D. S. Chen, I. Mellman, *Immunity* **2013**, *39*, 1-10.
[10] A. J. Muller, J. B. DuHadaway, P. S. Donover, E. Sutanto-Ward, G. C. Prendergast, *Nat. Med.* **2005**, *11*, 312-319.
[11] a) L. Kelland, *Nat. Rev. Cancer* **2007**, *7*, 573-584; b) D. Wang, S. J. Lippard, *Nat. Rev. Drug Discov.* **2005**, *4*, 307-320.
[12] L. Bracci, G. Schiavoni, A. Sistigu, F. Belardelli, *Cell Death Differ.* **2014**, *21*, 15-25.
[13] a) Q. Wang, D. O'Hare, *Chem. Rev.* **2012**, *112*, 4124-4155; b) B. Li, Z. Gu, N. Kurniawan, W. Chen, Z. P. Xu, *Adv. Mater.* **2017**, *29*, 1700373-n/a; c) N. Mitter, E. A. Worrall, K. E. Robinson, P. Li, R. G. Jain, C. Taochy, S. J. Fletcher, B. J. Carroll, G. Q. Lu, Z. P. Xu, *Nature Plants* **2017**, *3*, 16207; d) D.-H. Park, J. Cho, O.-J. Kwon, C.-O. Yun, J.-H. Choy, *Angew. Chem. Int. Ed.* **2016**, *55*, 4582-4586; *Angew. Chem.* **2016**, *128*, 4688-4688; e) R. Ma, Z. Wang, L. Yan, X. Chen, G. Zhu, *J. Mater. Chem. B* **2014**, *2*, 4868-4875.
[14] M. F. Cheng, M. S. Hung, J. S. Song, S. Y. Lin, F. Y. Liao, M. H. Wu, W. Hsiao, C. L. Hsieh, J. S. Wu, Y. S. Chao, C. Shih, S. Y. Wu, S. H. Ueng, *Bioorg. Med. Chem. Lett.* **2014**, *24*, 3403-3406.
[15] a) D. Y. Q. Wong, W. W. F. Ong, W. H. Ang, *Angew. Chem. Int. Ed.* **2015**, *54*, 6483-6487; *Angew. Chem.* **2014**, *126*, 6870-6874; b) E. Petruzzella, J. P. Braude, J. R. Aldrich-Wright, V. Gandin, D. Gibson, *Angew. Chem. Int. Ed.* **2017**, *56*, 11539-11544; *Angew. Chem.* **2017**, *129*, 11697-11702; c) J. S. Butler, P. J. Sadler, *Curr. Opin. Chem. Biol.* **2013**, *17*, 175-188; d) X. Wang, Z. Guo, *Chem. Soc. Rev.* **2013**, *42*, 202-224; e) Z. Wang, Z. Xu, G. Zhu, *Angew. Chem. Int. Ed.* **2016**, *55*, 15564-15568; *Angew. Chem.* **2016**, *128*, 15910-15910.
[16] Z. Wang, R. Ma, L. Yan, X. Chen, G. Zhu, *Chem. Commun.* **2015**, *51*, 11587-11590.
[17] U. F. Rohrig, S. R. Majjigapu, P. Vogel, V. Zoete, O. Michielin, *J. Med. Chem.* **2015**, *58*, 9421-9437.
[18] P. Hwu, M. X. Du, R. Lapointe, M. Do, M. W. Taylor, H. A. Young, *J. Immunol.* **2000**, *164*, 3596-3599.
[19] a) O. Takikawa, *Biochem. Biophys. Res. Commun.* **2005**, *338*, 12-19; b) S. Agaugué, L. Perrin-Cocon, F. Coutant, P. André, V. Lotteau, *J. Immunol.* **2006**, *177*, 2061-2071.
[20] B. Molon, B. Calì, A. Viola, *Front. Immunol.* **2016**, *7*, 20.
[21] X. Liu, N. Shin, H. K. Koblish, G. Yang, Q. Wang, K. Wang, L. Leffet, M. J. Hansbury, B. Thomas, M. Rupar, P. Waeltz, K. J. Bowman, P. Polam, R. B. Sparks, E. W. Yue, Y. Li, R. Wynn, J. S. Fridman, T. C. Burn, A. P. Combs, R. C. Newton, P. A. Scherle, *Blood* **2010**, *115*, 3520-3530.
[22] G. Ryan, *Nat. Rev. Immunol.* **2010**, *10*, 7-7.
[23] R. B. Holmgaard, D. Zamarin, D. H. Munn, J. D. Wolchok, J. P. Allison, *J. Exp. Med.* **2013**, *210*, 1389-1402.
[24] a) Z. Gu, H. Zuo, L. Li, A. Wu, Z. P. Xu, *J. Mater. Chem. B* **2015**, *3*, 3331-3339; b) Q. Chen, C. Wang, L. Cheng, W. He, Z. Cheng, Z. Liu, *Biomaterials* **2014**, *35*, 2915-2923; c) X. Song, C. Liang, H. Gong, Q. Chen, C. Wang, Z. Liu, *Small* **2015**, *11*, 3932-3941; d) J.-H. Lee, K. Lee, S. H. Moon, Y. Lee, T. G. Park, J. Cheon, *Angew. Chem. Int. Ed.* **2009**, *48*, 4174-4179; *Angew. Chem.* **2009**, *121*, 4238-4243.
[25] a) S. P. Patel, A. Bristol, O. Saric, X.-P. Wang, A. Dubeykovskiy, P. M. Arlen, M. A. Morse, *Cancer Immunol. Immunother.* **2013**, *62*, 1011-1019; b) S. Jang, Y. T. Kim, H. W. Chung, K.-R. Lee, J.-B. Lim, K. Lee, *Cancer* **2012**, *118*, 2173-2183; c) Z. Wang, T. Zhang, H. Hu, H. Zhang, Z. Yang, L. Cui, W. He, *Cancer Lett.* **2008**, *272*, 242-252.
[26] S. G. Awuah, Y. R. Zheng, P. M. Bruno, M. T. Hemann, S. J. Lippard, *J. Am. Chem. Soc.* **2015**, *137*, 14854-14857.
[27] R. Ma, Y. Wang, L. Yan, L. Ma, Z. Wang, H. C. Chan, S.-K. Chiu, X. Chen, G. Zhu, *Chem. Commun.* **2015**, *51*, 7859-7862.

10.1002/ange.201800422

WILEY-VCH

COMMUNICATION

An immuno-chemotherapy weapon: A cisplatin-loaded nanohybrid bearing inhibitors of indoleamine-2,3-dioxygenase significantly activates T cells, leading to cervical cancer cell cycle arrest and further increased cancer cell death.

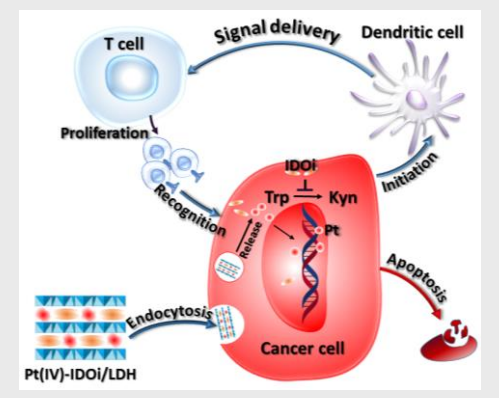

*Na Wang, Zhigang Wang, Zoufeng Xu, Xianfeng Chen, and Guangyu Zhu**

Page No. – Page No.

A cisplatin-loaded immuno-chemotherapeutic nanohybrid bearing immune checkpoint inhibitors for enhanced cervical cancer therapy

Supplementary Information

Table of Contents

Contents Page

Experimental Details

Materials and general instruments

All the related chemicals were acquired from commercial resources, except the IDO inhibitor was prepared following the reported protocols[1] and characterized by ^{1}H NMR and ^{13}C NMR. Trichloroacetic acid (TCA), *p*-Dimethylaminobenzaldehyde (Ehrlich's reagent), ethanol, D-1-methyl-tryptophan (D-1MT), L-tryptophan, L-kynurenine, glacial acetic acid, ethylenediaminetetraacetic acid (EDTA) and Triton X-100 were obtained from Sigma-Aldrich Pty Ltd. Dulbecco's modified eagle medium (DMEM), Roswell Park Memorial Institute 1640 (RPMI 1640) medium, minimum essential medium (MEM), trypsin, phosphate buffered saline (PBS), fetal bovine serum (FBS), non-essential amino acids (NEAA), sodium pyruvate, 3-(4,5-dimethyl-2-thiazolyl)-2,5-diphenyl-2H-tetrazolium bromide (MTT), recombinant human interferon-γ (hIFN-γ), propidium iodide (PI), 7-amino actinomycin D (7-AAD), annexin V-FITC, phytohemagglutinin-M (PHA-M), and CellTrace Far Red cell proliferation kit (carboxyfluorescein succinimidyl ester, CFSE) were obtained from Life Technologies. Bovine Serum Albumin (BSA) lyophilized powder was purchased from Acros Organics. IDO primary antibody (Cell Signaling Technology) and secondary antibody (Life Technologies) were purchased for western blotting. Flow cytometry experiments were performed at CytoFLEX S Flow Cytometer (Beckman). Peripheral blood mononuclear cells (PBMCs, Lonza) from unrelated healthy donators and FITC-conjugated anti-CD3 antibody (Abcam, ab34275) were purchased for flow cytometry. DeadEnd™ Fluorometric TUNEL System (G3250) was obtained from Promega Corporation, USA.

Synthesis of Pt(IV)/LDH, IDOi/LDH, Pt(IV)-IDOi/LDH

Cisplatin prodrug *c,c,t*-$[Pt(NH_3)_2Cl_2(O_2CCH_2CH_2COOH)_2]$ (DSCP), IDO inhibitor 4-{[2-(4-Bromophenyl)hydrazinyl]sulfonyl}benzoic acid (IDOi) and layered double hydroxides (LDH) were prepared following the reported literatures[2] and our previous work,[3] respectively. Pt(IV)/LDH was synthesized as the previous reports[4]. Briefly, 1.5 mL DSCP (5 mM, pH 8.0) and LDH were stirred together overnight, and the synthesized suspension was washed twice with Milli-Q water for further study. For the synthesis of IDOi/LDH, IDOi (20 mM, 1.325mL, pH 8.0) was added to a suspension of LDH nanoparticles (4.0 mg/mL, 1.0 mL) and stirred overnight in dark. The complex was then washed twice with 12,000 × g centrifugation for 10 min and resuspended in Milli-Q water. Pt(IV)-IDOi/LDH with different ratios of Pt(IV) and IDOi were synthesized through a similar process. 500 μL DSCP (5 mM) and various amount of IDOi were added in LDH nanoparticles suspension before stirred overnight. All the prepared samples were stored at 4°C in dark.

Characterization of nanoparticles

The Pt content in the nanoparticles was determined by Inductively Coupled Plasma Optical Emission Spectrometry (ICP-OES, PerkinElmer, Optima 8000). UV-vis spectroscopy (Shimadzu, UV-1700 PharmaSpec, UV-vis Spectrophotometer) was applied to quantify the amount of IDOi in the nanoparticles. Transmission Electron Microscopy (TEM, Philips Technai 12) was employed for morphology analysis. The size distribution and zeta potential were measured by dynamic light scattering (DLS) on Malvem Zetasizer Nano ZS.

Pt and IDOi content in nanoparticles

Pt release level in each sample (100μL) was digested by 400 μL concentrated nitric acid overnight, then the mixture was diluted with 500 μL DI water before ICP-OES measurement. The nanoparticles (100 μL) were pretreated with 0.1 N HCl

(900 μL) overnight to break down LDH and to release free IDOi before UV-vis spectroscopy measurements. The absorbance peak of IDOi at 230 nm was employed to calculate the concentration of IDOi in the digested solution.

Cell lines and cell culture conditions

HeLa, MCF-7, A549 and A549cisR cells were maintained in DMEM with 10% FBS and 50 U/mL penicillin and streptomycin. A2780 cells were maintained in RPMI 1640 with 10% FBS, 2 mM L-glutamine and 50 U/mL penicillin and streptomycin. WI-38 cells (human lung fibroblast) were maintained in MEM with 10% FBS, 1% L-glutamine, 1% NEAA and 1% sodium pyruvate. Human cervical epithelial cells (HCvEpC) were obtained from Cell Applications, Inc., and maintained in Epithelial Cell Growth Medium (Cell Applications, Inc., USA). A kind of special medium (10% dextrose, 40% RPMI and 50% FBS) was applied to thaw the PBMCs and the cells were consequently cultured in RPMI complete culture medium (20% FBS). To mimic *in vivo* circumstances, the processes to change the medium in PBMCs culture flask were modified as described: half of the culture medium was taken out from the flask, then the supernatant was discarded after centrifugation, the cell pellet was resuspended in fresh medium and mixed with the original half volume of PBMCs in the flask. With the purpose of keeping some growth factors or cytokines inside, the procedure will lose a few PBMCs after medium changed undoubtedly. All the cells were grown in a humidified incubator at 37˚C with 5% carbon dioxide.

Western blotting

MCF-7, HeLa, A2780, A549, A549cisR, WI-38, MRC-5, and HCvEpC cells (1×10^6 cells) were incubated with or without hIFN-γ (50 ng/mL) in 10 cm petri dish for 3 days at 37˚C. Cells were washed with cold PBS for twice. Cells were scraped and lysed, then quantified and mixed with loading buffer. The whole cell lysates were applied in sodium dodecylsulphate polyacrylamide gel electrophoresis (SDS-PAGE, 10% resolving gel and 15% stacking gel) at 70 V for about 150 min, and transferred to polyvinylidene difluoride membrane (PVDF) with 700 mA for 60 min. Membranes were subsequently blocked with 5% (w/v) nonfat milk powder in TBST (Tris buffer saline with 0.1% tween-20) for 1 h at room temperature and incubated with the IDO primary antibody (Cell signaling Technology) overnight. The membranes washed with 4% milk Tris buffer saline for 3 to 5 times. After incubation of horseradish peroxidase conjugated secondary antibody (Thermo Scientific) for 1h, the membrane was washed with TBST for 3 to 5 times, followed by ECL reagent (Thermo Scientific) and imaged with Bio-Red ChemiDoc™ Touch Imaging System.

Cell viability tests

MTT assay was employed to measure the cell viability. HeLa, A549, WI-38 cells (3×10^3 cells/well) and HCvEpC (6.5×10^3 cells/well) were seeded in 96-well plates and incubated overnight. The fresh medium containing various concentrations of complexes was subsequently added when the cells reach about 30% confluency in each well. 72 h later, the medium in each well was replaced by the serum-free medium containing 1 mg/mL MTT. After 1 h of incubation, 200 μL DMSO was added after the removal of medium to dissolve the formazan in each well. The absorption of 550 nm and 700 nm was measured in a microplate reader. The viability of PBMCs (100 μL) from different treatment conditions was determined by using the MTS (3-(4,5-dimethylthiazol-2-yl)-5-(3-carboxymethoxyphenyl)-2-(4-sulfonyl)-2H-tetrazolium) reagent (Promega Corporation, USA).

Cellular accumulation of platinum in HeLa cells

HeLa cells were seeded in 10 cm petri dishes and incubated until the cell confluency reached 80%. The medium was changed to fresh medium containing cisplatin, cisplatin with IDOi (1:40), Pt(IV)/LDH and Pt(IV)-IDOi(1:40)/LDH at the concentration of 5 and 10 μM Pt. After 8 h, cells were collected and washed with ice-cold PBS for 3 times. Cell pellet was resuspended in 1 mL PBS. The cells were then digested by 30% conc. nitric acid overnight at 65˚C, and the Pt content was measured by ICP-OES. The platinum level in cells was expressed as ng Pt per 10^6 cells.

Pt level in Genomic DNA

HeLa cells were seeded in 10 cm petri dishes and incubated until the cell confluency reached 80%. The medium was changed to fresh medium containing cisplatin, cisplatin with IDOi (1:40), Pt(IV)/LDH and Pt(IV)-IDOi(1:40)/LDH at the concentration of 5 and 10 μM Pt. After 8 h of incubation, cells were harvested, counted, and washed with ice-cold PBS for 3 times. The cell pellet was resuspended in 2 mL of a lysing buffer (100 mM Tris-HCl, pH 8.5, 5 mM EDTA, 0.2% SDS, 200 mM NaCl, 100 μg/mL proteinase K) and incubated overnight at 55˚C. The samples were extracted twice with 2 mL of phenol/chloroform/isoamyl alcohol (25:24:1) (vortex and centrifugation at 4,500 rpm, 5 min). The supernatant was transferred to a new tube, and followed by two extractions with chloroform. Genomic DNA was precipitated with 0.7 × sample volume of isopropanol, then washed with 0.7 × sample volume of ice-cold ethanol (70%) twice, centrifuged at 15,000 rpm for 25 min. The DNA pellet was dissolved in 10 mM Tris/HCl (pH 8.0) buffer (10 mM tris, 1 mM EDTA, 50 μg/mL RNase). The DNA concentration was quantitated by UV-vis spectroscopy. The amount of platinum on the DNA was determined by ICP-OES. The concentration of platinum was expressed as ng of platinum per 10^6 cells.

Cell-based kynurenine assay

HeLa cells were seeded in 48-well plates at a density of 3×10^4 cells/well. Then all the medium was removed on the next day. The hIFN-γ (25 ng/mL as final concentration) and various concentrations of complexes were added in a total volume of 200 μL of culture medium containing 100 μM of L-tryptophan. After 48 h of incubation, 140 μL supernatant in each well was transported into the 96-well plates and mixed with 15 μL of 30% TCA. The mixture was incubated for 30 min at 50˚C. The microplates were then centrifuged for 10 min at 3,000 × g to remove the sediments. 100 μL of the supernatant was mixed with 100 μL of 2 % (w/v) *p*-dimethylaminobenzaldehyde in acetic acid and measured at 480 nm in a microplate reader. The concentration of kynurenine in each sample was quantified from a kynurenine standard curve.

T cell proliferation in HeLa/MLRs

HeLa cells were seeded with a density of 1×10^3 cells/well in 6-well plates. Twenty-four hours after the HeLa cells cultivation, the medium in each well was replaced with 2 mL fresh complete DMEM containing various concentrations of complexes, 50 ng/ml IFN-γ and 0.1 mM L-tryptophan. The HeLa cells were exposed to different complexes for 2 d with Pt concentration is 0.04 μM. PBMCs (2×10^5 cells/well) stained with CellTrace™ Far Red Cell Proliferation Kit (CFSE) were subsequently inserted after PHA-M stimulation. After 6 days of co-culture, the PBMCs in each well were collected after centrifugation, the cell pellets were resuspended in PBS and labeled with FITC-conjugated anti-CD3 antibody. With cell staining finished, all the samples were collected and analyzed by flow cytometry. T cell proliferation analysis was implemented on CytoFLEX S flow cytometer (Beckman Coulter, USA). All the samples were tested with the excitation light of 630 nm and detected emission at 661 nm for CellTrace Far Red (CFSE) stained PBMCs, the excitation and emission wavelengths at 495 nm/519 nm were detected simultaneously for cells bound with FITC-conjugated anti-CD3. Signals from 10,000 events were collected for each sample. Based on the flow cytometric data, the T cell proliferation

in each sample was analyzed by FlowJo software. The dual-staining positive cells were taken as valid data in each sample.

Flow cytometry protocol of cell gating: for the test of T cell proliferation in each sample, PBMCs were first stained with CFSE and labeled with FITC-conjugated anti-CD3 antibody six days later as described above. Then the PBMCs cells were analyzed by flow cytometer. For the analysis of data, FlowJo software was used. To determine the gate of proliferation T cells, three additional groups were included: a) the PBMCs without staining CFSE and FITC-conjugated anti-CD3 antibody; b) CFSE stained PBMCs, and c) FITC-conjugated anti-CD3 antibody labeled PBMCs. FL3 channel was set as the x-axis, FL1 channel was set as the y-axis. For $CFSE^+$ cells, the gate was adjusted that $FITC^-$ but $CFSE^+$ cells were displayed in the lower right quadrant. Similar gating way in $CD3^+$ cells, gates were placed in such a way that $FITC^+$ but $CFSE^-$ cells were displayed in the upper left quadrant, leaving the double-stained positive cells in the upper right quadrant, and the double-unstained cells in the lower left quadrant. Gates were kept for all samples. Only the upper right quadrant ($FITC^+$, $CFSE^+$) of each sample was selected as T cells and applied for T cell proliferation analysis. The proliferation of T cells was analyzed with FlowJo's Proliferation Tool. FL3 channel was set as the x-axis, and the y-axis was Histogram. FlowJo modeled the division by looking for peaks with diminishing fluorescence with a ratio of 0.5 per generation.

Cell cycle analysis for HeLa cells

HeLa cells were cultured in 6-well plates with a density of 3×10^3 cells/well. 1×10^5 PBMCs were added into the HeLa cells with or without compounds ([Pt] = 5 μM). After 6 days of incubation, suspended PBMCs were removed and the HeLa cells were washed twice with PBS for cell cycle analysis. HeLa cells were then harvested and washed twice with PBS with centrifugation, 1,500 rpm/5 min. The cell pellets were resuspended in 0.5 mL PBS and fixed in 5 mL ethanol (70%) at 4˚C overnight. Then the fixed cells were washed after centrifugation, and resuspended in 1 mL PI solution (0.1% Triton X-100, 200 μg/mL RNase A, 20 μg/mL propidium iodide, pH 7.4). The cells were incubated at 37°C for 30 min in dark. Cell cycle distribution was analyzed by a BD flow cytometer with excitation at 488 nm and emission at 632 nm. The data were analyzed by a FlowJo 7.6.1 software.

Apoptosis analysis in HeLa cells using flow cytometry

HeLa cells were seeded in 6-well plates at a density of 1×10^4 cells per well and incubated for 24 h. Pt(IV)-IDOi(1:40)/LDH ([Pt] = 5 μM) were added with/without PHA-M activated PBMCs (3×10^5 cells/well). After 72 h of incubation, HeLa cells were harvested for apoptosis analysis. The cells were subsequently washed with cold PBS and annexin binding buffer, and the cell density was determined and adjusted to 1×10^6 cells per mL. Annexin V conjugated FITC and 7-AAD solution were added to 100 μL cells suspension. The cells were stained at RT for 15 min, then 400 μL annexin binding buffer was added and mixed gently. The as-prepared samples were kept on ice and analyzed by flow cytometer with excitation at 488 nm and emission at 532 nm and 650 nm for FITC and 7-AAD, respectively.

Apoptosis analysis in HeLa cells using TUNEL

HeLa cells (1×10^4) were seeded on slides and incubated for 24h before Pt(IV)-IDOi(1:40)/LDH ([Pt] = 5 μM) were added with/without PHA-M activated PBMCs (3×10^5). After 3 days of incubation, HeLa cells on the slides were fixed in 4% formaldehyde in PBS for 25 min at 4˚C, and washed twice in PBS. Sides were immersed in 0.2% Triton X-100 in PBS for 5 min for permeabilizing cells. Then cells equilibrated with 100 μL Equilibration Buffer at room temperature for 5-10

min, and labeled with 50 μL TdT reaction mix (45 μL Equilibration Buffer, 5 μL Nucleotide Mix and 1 μL rTdT Enzyme) at 37˚C for 60 min in a humidified chamber. Slides were protected from light since this step forward. Stop label reaction by immersing slides in 2 X SSC buffer, slides were washed three times with PBS to remove unincorporated fluorescein-12-dUTP. To visualize all nuclei, freshly prepared PI working solution (1 μg/mL propidium iodide, in PBS) was applied to counterstain all samples. Samples were immediately analyzed under a motorized fluorescence microscope (Nikon Eclipse 90i). Apoptotic cells with green fluorescence were detected at 520 nm, and the nuclei with red fluorescence were viewed at 620 nm. ImageJ software was used for quantification. For the TUNEL result, the apoptotic index was expressed as the percentage of TUNEL-positive cells out of the total number of cells counted.

Pt accumulation in HeLa, PBMCs, T cells and medium for delivery efficiency test

HeLa cells (1 x 10^4) were seeded in 6-well plates and incubated for 24h following the addition of Pt(IV)-IDOi(1:40)/LDH ([Pt] = 5 μM) with/without PHA-M activated PBMCs (3 × 10^5). After 72 h of incubation, PBMCs in each well were harvested and washed three times with ice-cold PBS, and resuspended in 1 mL PBS. The Pt accumulation in T cells was tested after sorting: the incubated PBMCs in HeLa/MLRs were washed three times with PBS, and sorted with SH800 Cell Sorter (Sony Biotechnology) after labeled with a FITC-conjugated anti-CD3 antibody. The PBMCs and sorted T cells were then digested by 30% conc. nitric acid overnight at 65˚C, and the Pt content was measured by ICP-MS (PerkinElmer Nexion 2000). The platinum level in cells was expressed as ng Pt per 10^6 cells. The delivery efficiency test was carried in three different conditions: a) HeLa + Pt(IV)-IDOi(1:40)/LDH ([Pt] = 5 μM); b) HeLa + Pt(IV)-IDOi(1:40)/LDH ([Pt] = 5 μM) + PBMCs; and c) Pt(IV)-IDOi(1:40)/LDH ([Pt] = 5 μM) + PBMCs. After 72 h of incubation, HeLa cells, supernatant in each well, and PBMCs were harvested for the ICP-MS test as above.

Preparation of BSA-coated nanohybrid

Albumin-coated nanoparticles were synthesized for the *in vivo* experiment[5]. In brief, 5 mL suspension of as-prepared Pt(IV)-IDOi(1:40)/LDH was added into 5 mL BSA stock solution (10 mg/mL) dropwise with the albumin/ LDH mass ratio of 5 : 2 under vigorous stirring. The reaction was stirred for 30 min and protected from light. After the reaction, the BSA-coated nanohybrid was washed 3 times with PBS and re-suspended in PBS for *in vivo* experiment.

Characterization of nanohybrid and BSA-coated nanohybrid in blood plasma

Whole blood was collected from healthy BALB/c nude mice into the EDTA-treated microtube. Then the cells were removed from plasma by centrifugation for 15 min at 2,000 x g, 4˚C. To check the characterization of nanoparticles in blood plasma, centrifuged nanoparticles or BSA-coated nanoparticles (12,000 x g, 10 min) were dispersed in 300 μL mice blood plasma. After 5 s of vortex, 100 μL of blood plasma and nanohybrid mixture were taken out and washed twice with PBS (12,000 rpm, 10 min) for characterization at 0 h. The rest mixture was maintained in 37 ˚C for 24 h. TEM, size distribution and zeta potential of the samples were taken for the characterization

***In vivo* anti-tumor efficacy in subcutaneous HeLa xenograft mouse model**

To evaluate the immune-chemotherapeutic nanohybrid, an anti-tumor efficacy model was established on BALB/c background nude mice. The HeLa cervical cancer cells (5 × 10^5 cell / 0.1 mL / mouse) were subcutaneously implanted in the right axillary fossa of BALB/c nude mice (6-week-old, 18 - 23 g body weight) to establish the xenograft mouse

model. Tumor nodules were allowed to grow 7 days to achieve a diameter of 5 - 8 mm before treatment initiation. All the mice were numbered with ear tags. The treatment phase included intravenously injection of PHA-M-activated normal PBMCs (approximately 5 x 10^6 cell / 0.1 mL / mouse), followed on intravenously injection of BSA-coated Pt(IV)-IDOi(1:40)/LDH ([Pt] = 0.5 mg/kg) and PBS as a negative control (Figure S12). The BSA-coated nanohybrid was injected every two days for total four times of injection. Since HeLa cells grow aggressively in nude mice, the experiment is terminated on Day 14. The tumor dimension and body weight were measured every two days for 14 days of duration. Tumor length and width were measured with calipers, and the tumor volume was calculated using the following equation: $TV=(a)(b^2)\pi/6$, where a is the longest dimension and b is the largest dimension orthogonal to a. Statistical analysis was performed using Student's t-Test at the end point.

Determination of tryptophan and kynurenine level in tumor by high-pressure liquid chromatography (HPLC)

All the mice in each group were sacrificed after experiment terminated, tumors were harvested and frozen at -80 ˚C after washed in phosphate-buffered saline. The total free tryptophan and kynurenine in tumors were quantified by HPLC[6]. The tumors were homogenized with ice-cold 0.16 M perchloric acid containing 0.1% EDTA and 0.1% ascorbic acid for 5 min and centrifuged at 20,000 x g for 20 min, and the supernatant was filtered for HPLC. The chromatography was performed in a Shimadzu LC-20AT liquid chromatograph with a 250- by 4.6-mm (inner diameter) C18 reverse-phase column (Phenomenex, Gemini 5 µ C18 110A). In tryptophan measurement, the column was eluted at a flow rate of 1.0 ml/min with 0.015 M sodium acetate (pH 4.5) containing 15% methanol for analysis of tumor samples. For kynurenine determination, the column was eluted with acetonitrile at a 1:47 dilution in 0.1 M acetic acid-0.1 M ammonium acetate (pH 4.65). The absorbance of the column effluent was monitored at 280 and 365 nm for tryptophan and kynurenine, respectively. The peaks of tryptophan or kynurenine were identified by comparison with the retention time of standard compounds (Sigma), and quantification was based on the ratios of the peak areas of the compound to the standard.

Animal ethics

All BALB/c nude mice were purchased from the Chinese University of Hong Kong and maintained under pathogen-free conditions in the City University of Hong Kong. The studies involving animal all in accordance with the protocol and was approved by the Institutional Animal Ethics Committee.

Statistical analysis

All the results were expressed as Mean ± SD where applicable. GraphPad Prism 6 software (GraphPad Software) was used for statistical analysis. All the results are expressed as Mean ± SD.

Results

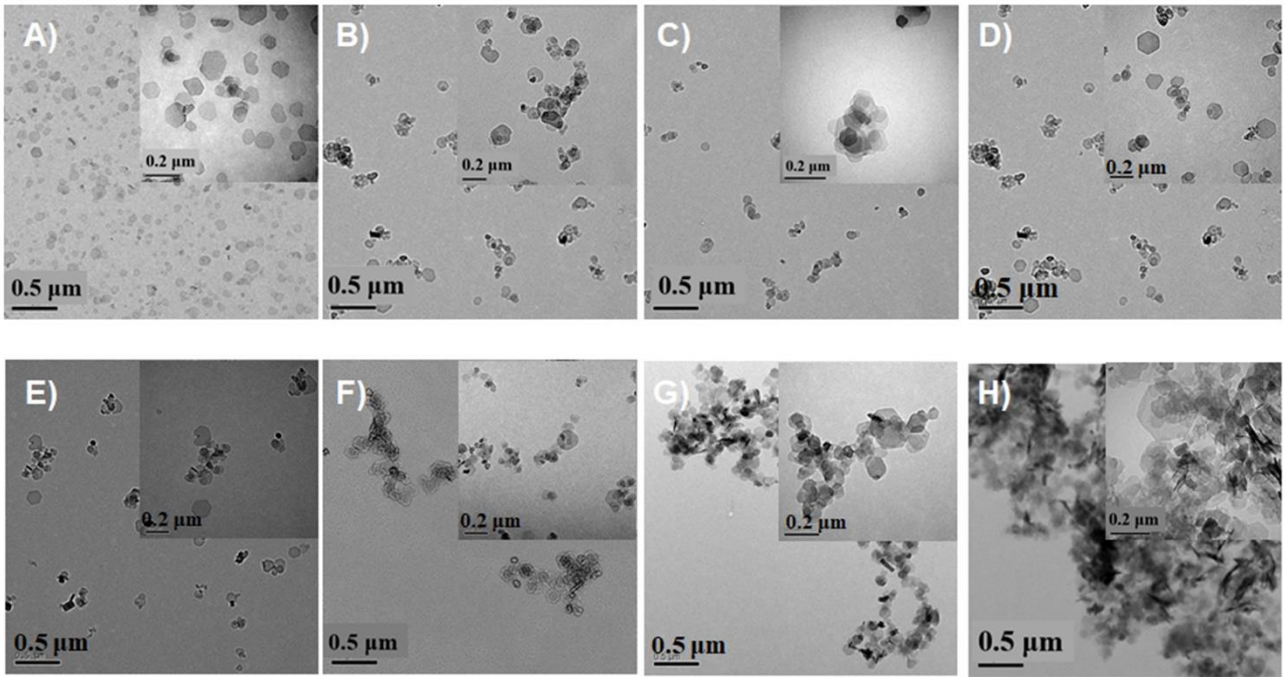

Figure S1. TEM images of A) LDH; B) Pt(IV)/LDH; C) IDOi/LDH; D) Pt(IV)-IDOi(10:1)/LDH; E) Pt(IV)-IDOi(1:2)/LDH; F) Pt(IV)-IDOi(1:10)/LDH; G) Pt(IV)-IDOi(1:40)/LDH; H) Pt(IV)-IDOi/LDH (1:245).

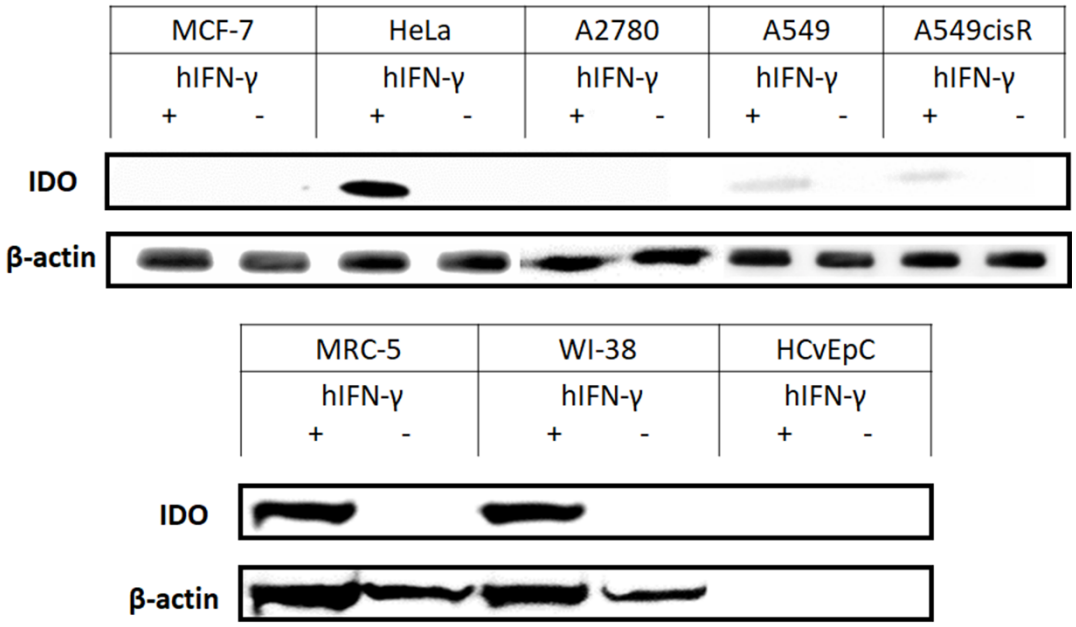

Figure S2. Western blot of IDO expression level with/without hIFN-γ stimulation. MCF-7, HeLa, A2780, A549, A549cisR, WI-38, MRC-5, and HCvEpC cells were seeded in 10 cm dish with/without hIFN-γ for 3 days, then the cells were collected for western blot.

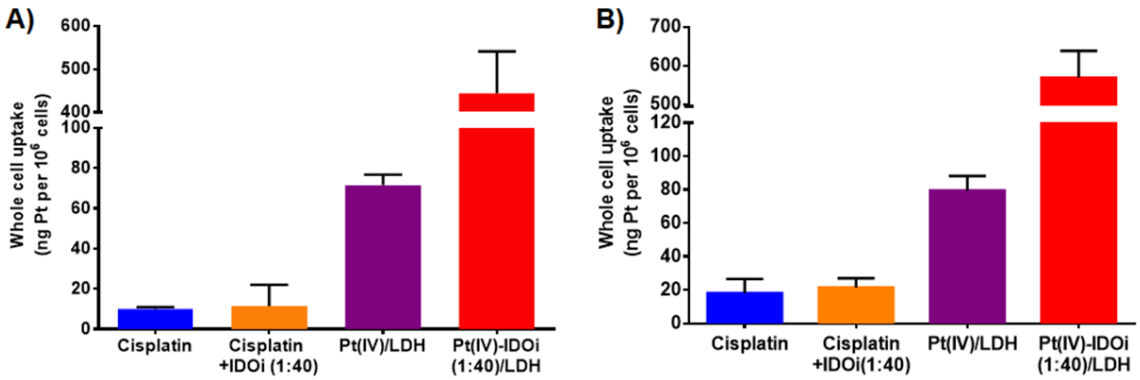

Figure S3. Cellular accumulation of Pt in HeLa cells. The Pt concentration in each sample is 5 μM in A) and 10 μM.in B). HeLa cells were treated with cisplatin, cisplatin + IDOi (1:40), Pt(IV)/LDH and Pt(IV)-IDOi(1:40)/LDH for 8 h. Mean ± SD.

To evaluate the efficient delivery and activation of Pt in HeLa cells, Pt accumulation in cells was assessed by ICP-OES. HeLa cells treated with cisplatin or cisplatin together with IDOi have similar intracellular levels of Pt (Figure S3). Pt(IV)/LDH and Pt(IV)-IDOi(1:40)/LDH ([Pt] = 5 μM) show significantly elevated levels of Pt compared with the small-molecule itself, and the levels are 71.5 ± 5.3 and 443.7 ± 97.3 ng per 10^6 cells, respectively, suggesting the efficient delivery of Pt by the nanoparticles. We also measured the Pt level in the genomic DNA of the treated HeLa cells. A 15-fold increase in genomic DNA is observed for Pt(IV)-IDOi(1:40)/LDH compared with cisplatin (Figure S4). These data clearly indicate the effective entrance of the Pt(IV) prodrug in Pt(IV)-IDOi/LDH into cancer cells and the efficient activation of the prodrug for damaging genomic DNA.

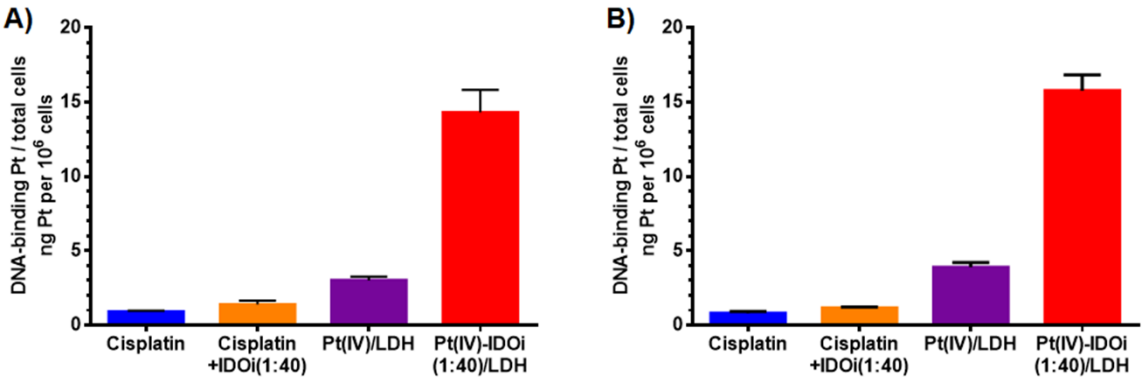

Figure S4. Pt levels of genomic DNA in total HeLa cells. The Pt concentration in each sample is 5 μM in A) and 10 μM.in B). HeLa cells were treated with cisplatin, cisplatin + IDOi (1:40), Pt(IV)/LDH, and Pt(IV)-IDOi(1:40)/LDH for 8 h. Mean ± SD.

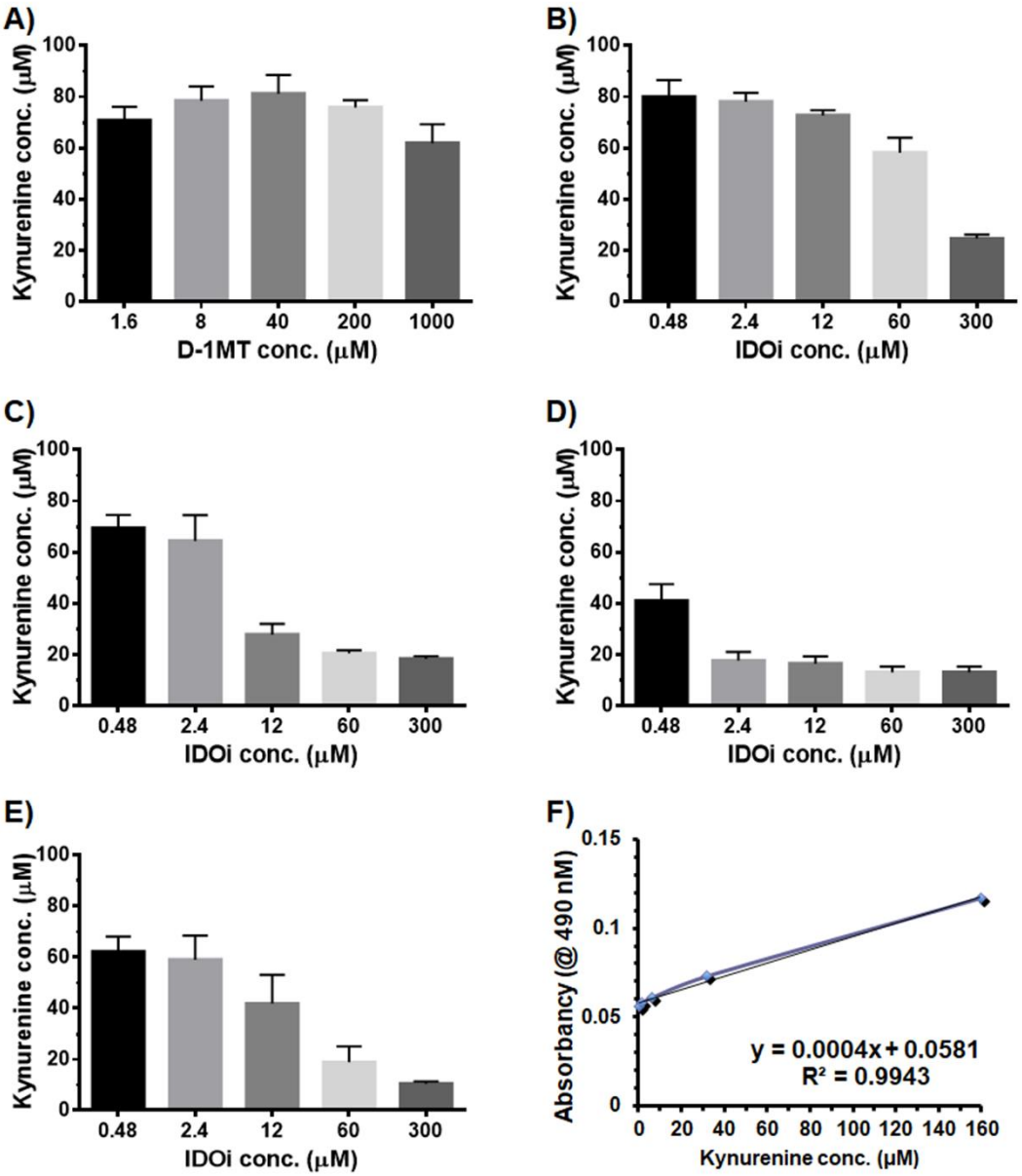

Figure S5. Inhibitory effect of A) D-1MT, B) IDOi, C) IDOi/LDH, D) Pt(IV)-IDOi(1:40)/LDH, and E) cisplatin + IDOi (1:40) on the level of kynurenine in HeLa cells after 48 h treatment containing hIFN-γ (25 ng/mL). The concentrations of complexes were added as indicated. Kynurenine concentrations were calculated using a F) kynurenine standard curve. Mean ± SD.

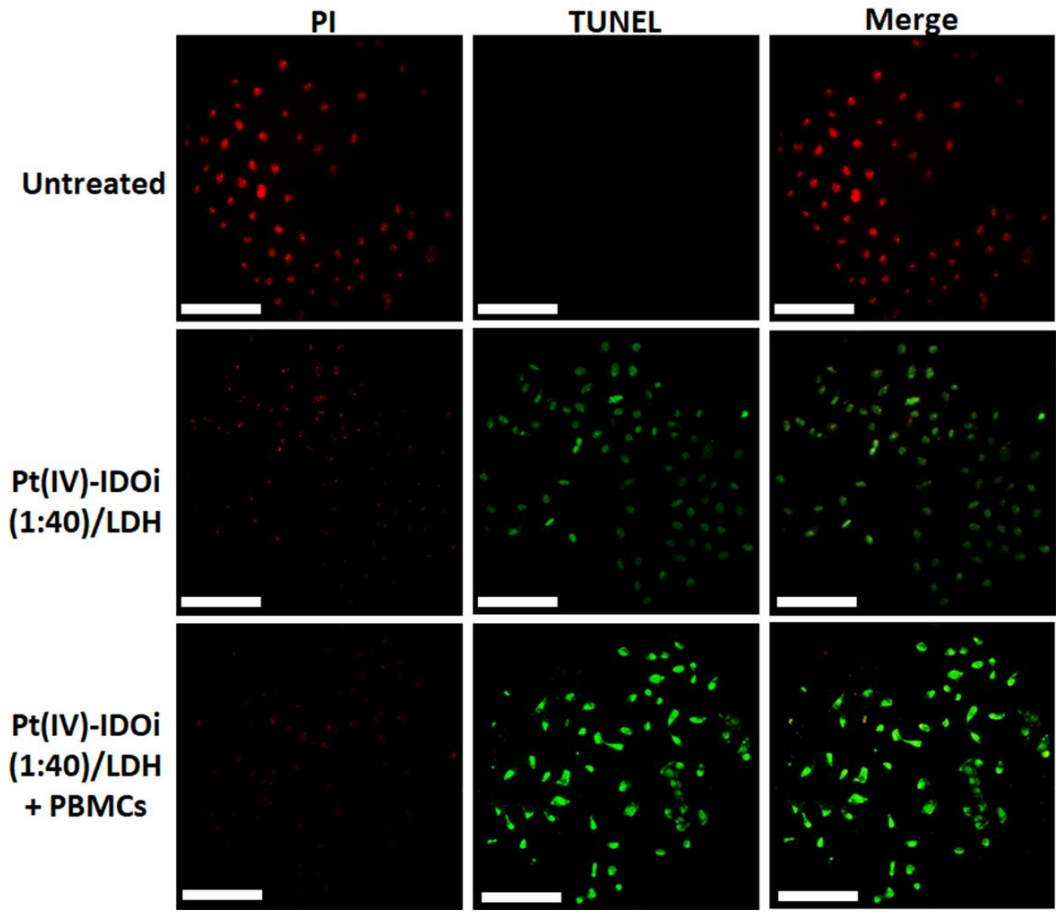

Figure S6. The apoptotic levels of HeLa cells in the HeLa/MLRs system tested by TUNEL assay. The concentration of Pt in the treatment is 5 μM. After 3 days incubation, all the samples were analyzed by a fluorescence microscope. Double staining samples of TUNEL (green) and PI (red) were viewed at 520 and 620 nm, respectively. All scale bars are 200 μm.

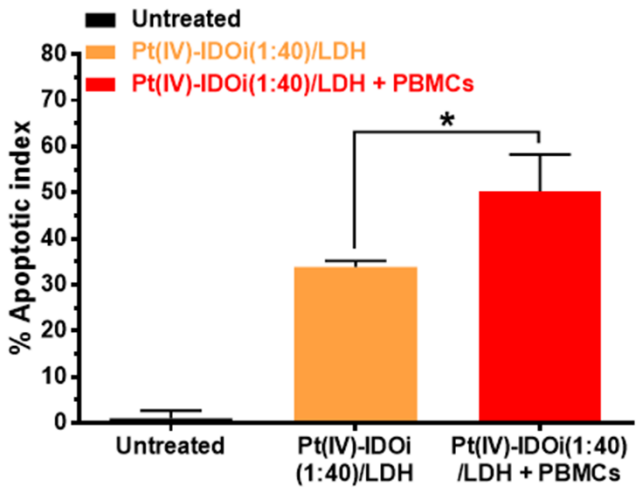

Figure S7. The apoptotic index (%) of HeLa cells in HeLa/MLRs. For the quantification of TUNEL assay, the apoptotic index was expressed as the percentage of TUNEL-positive cells out of the total number of cells counted. The treatment conditions for HeLa cells were: untreated, Pt(IV)-IDOi(1:40)/LDH ([Pt] = 5 μM), and Pt(IV)-IDOi(1:40)/LDH ([Pt] = 5 μM) + PBMCs for 3 days of culture. * $p < 0.05$. Mean ± SD.

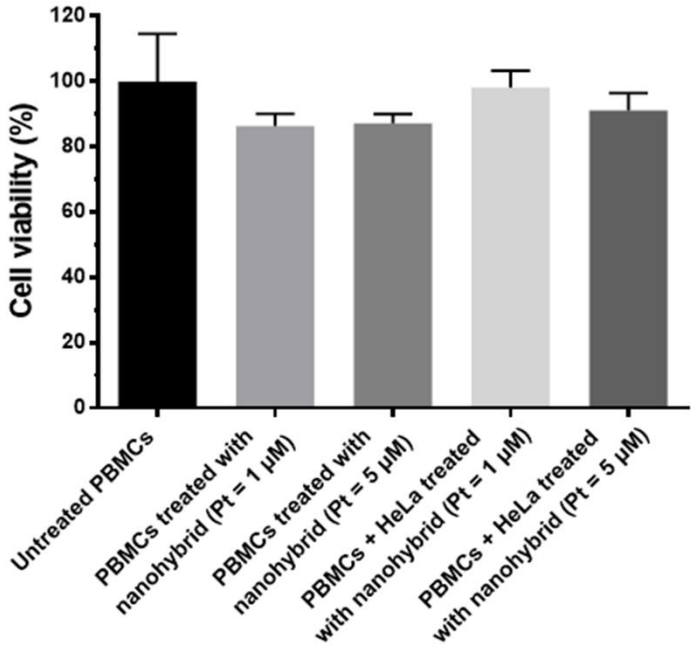

Figure S8. Cell viability (%) of PBMCs determined by MTS assay. The PBMCs were treated with Pt(IV)-IDOi(1:40)/LDH for 72 h in and without the presence of HeLa cells. Mean ± SD.

The possibility of unintended or off-target effects of the nanohybrid was further investigated in the co-culture system. Cell viability of PBMCs was first tested in different treatment conditions using an MTS assay (Figure S8). The cell viabilities of PBMCs do not significantly change after exposure to the nanohybrid ([Pt] = 1 or 5 μM) for 3 days in and without the presence of HeLa cells, indicating that our nanohybrid hardly affects the viability of T cells, the major component of PBMCs.[7] Distributions of the nanohybrid in HeLa cells and PBMCs were quantified (Figures S9 - S10). After treatment for 72 h ([Pt] = 5 μM), the percentage of Pt in HeLa cells, PBMCs, and supernatant is 27.0%, 4.6%, and 68.4%, respectively (Figure S9A), indicating that the nanohybrid is able to efficiently deliver Pt into HeLa cells rather than PBMCs.

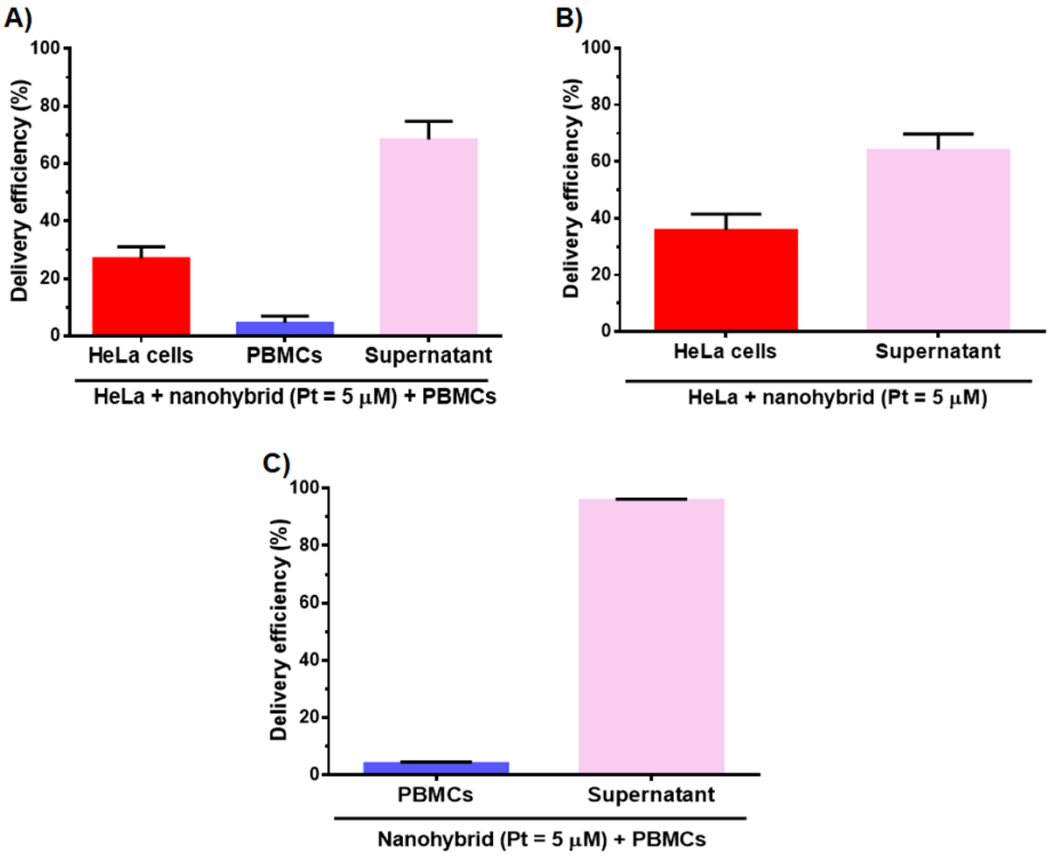

Figure S9. Delivery efficiency (%) of Pt(IV)-IDOi(1:40)/LDH under 3 different treatment conditions for 72 h: A) HeLa + PBMCs + nanohybrid ([Pt] = 5 μM); B) HeLa + nanohybrid ([Pt] = 5 μM); and C) PBMCs + nanohybrid ([Pt] = 5 μM). The data was tested by ICP-MS to quantify the Pt level in HeLa cells, supernatant, and/or PBMCs. Nanohybrid is Pt(IV)-IDOi(1:40)/LDH. Mean ± SD.

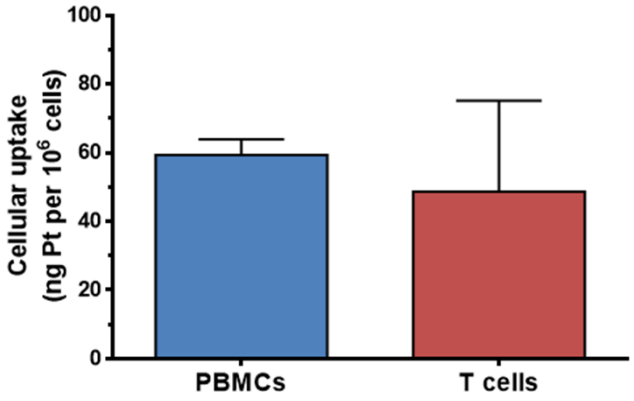

Figure S10. Cellular accumulation of Pt in PBMCs and T cells. The PBMCs in HeLa/MLRs system were treated with Pt(IV)-IDOi/LDH ([Pt] = 5 μM) for 3 days. After incubation, the PBMCs in each sample were harvested for cellular Pt accumulation test. The T cells were tested after cell sorting and quantified the Pt levels in the same way. Mean ± SD.

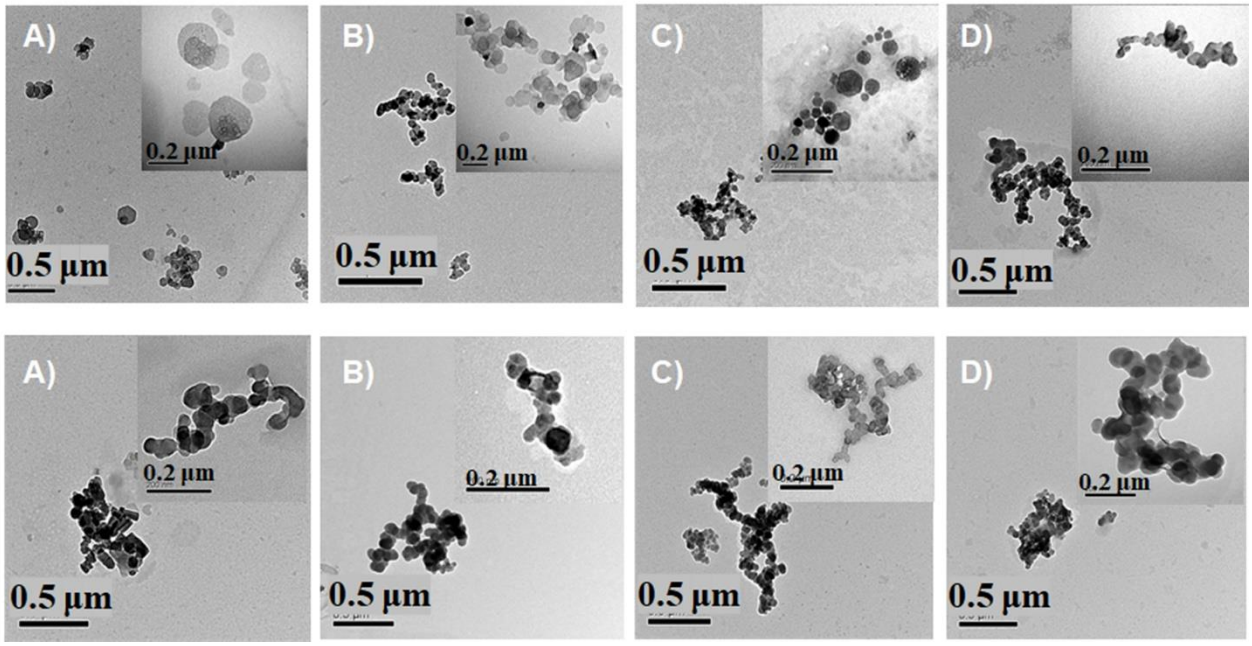

Figure S11. TEM images of nanoparticles incubated with blood plasma. Centrifuged nanoparticles were dispersed in fresh mice blood plasma. After vortex for 5 s, the TEM images were recorded for the mixture of blood plasma with A) LDH; B) Pt(IV)/LDH; C) IDOi/LDH; D) Pt(IV)-IDOi(1:40)/LDH. The rest of the samples was maintained in 37 ˚C for 24 h. TEM images were then achieved for the mixture of blood plasma with E) LDH; F) Pt(IV)/LDH; G) IDOi/LDH; H) Pt(IV)-IDOi(1:40)/LDH.

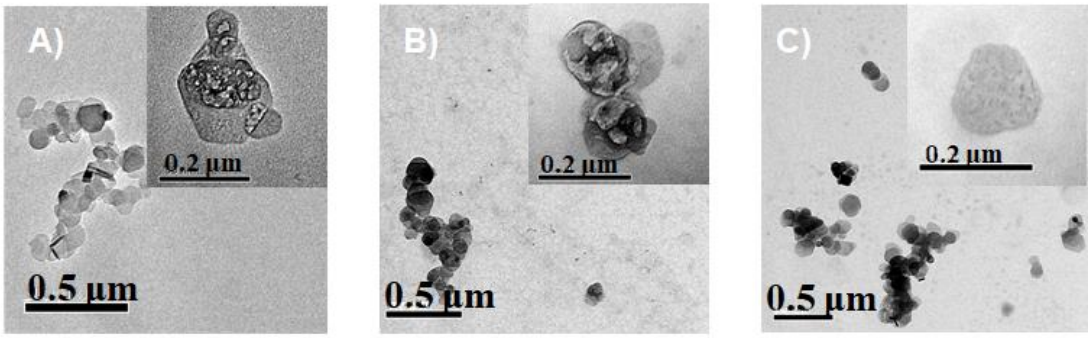

Figure S12. TEM images of BSA-coated nanoparticles in PBS or incubated with blood plasma. A) BSA-coated Pt(IV)-IDOi(1:40)/LDH in PBS, B) BSA-coated Pt(IV)-IDOi(1:40)/LDH incubated with blood plasma and monitored at 0 h, and C) BSA-coated Pt(IV)-IDOi(1:40)/LDH incubated with blood plasma at 37 ºC and observed at 24 h.

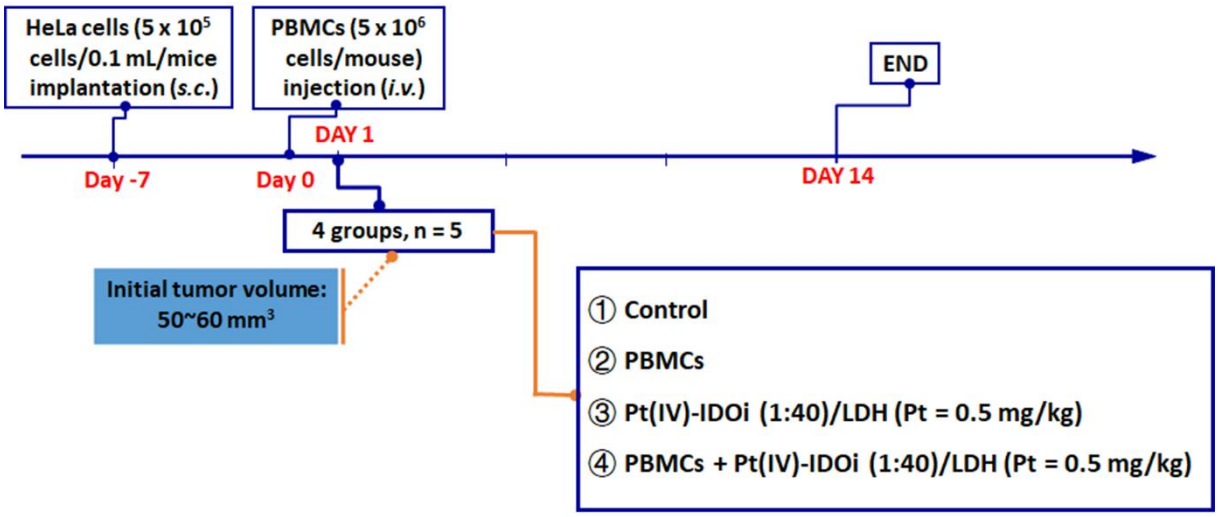

Figure S13. The schedule of *in vivo* experiment to evaluate the immune-chemotherapeutic nanohybrid. HeLa cervical cancer cells (5×10^5 cell / 0.1 mL / mouse) were subcutaneously implanted in BALB/c nude mice at Day -7 to establish the xenograft mouse model (n = 5). When the tumor masses achieved a diameter of 5 - 8 mm, PBMCs (5×10^6 cell / 0.1 mL / mouse) were intravenously injected, then BSA-coated Pt(IV)-IDOi(1:40)/LDH ([Pt] = 0.5 mg/kg) was injected and PBS was set as a negative control. The tumor dimension and body weight were measured every two days for total 14 days of duration.

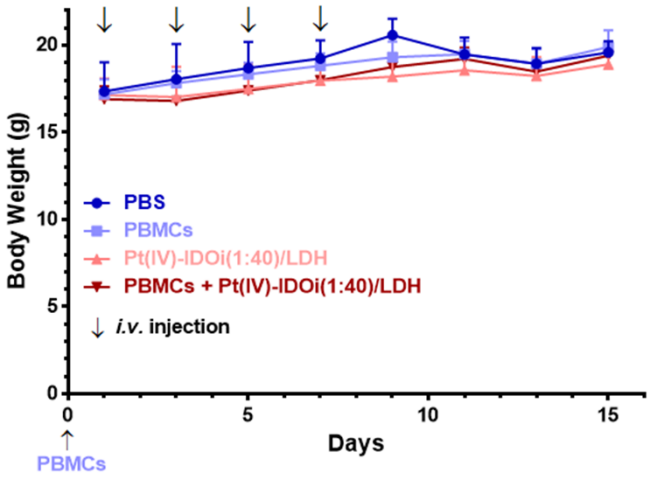

Figure S14. The change of body weight in 14 days after various treatment indicated. The PBMCs (5 x 10^6 cells/mouse) were injected intravenously at Day 0. BSA-coated Pt(IV)-IDOi(1:40)/LDH ([Pt] = 0.5 mg/kg) was injected for total 4 injection. The body weight of each group was measured every two days for 14 days of duration. Mean ± SD, n = 5.

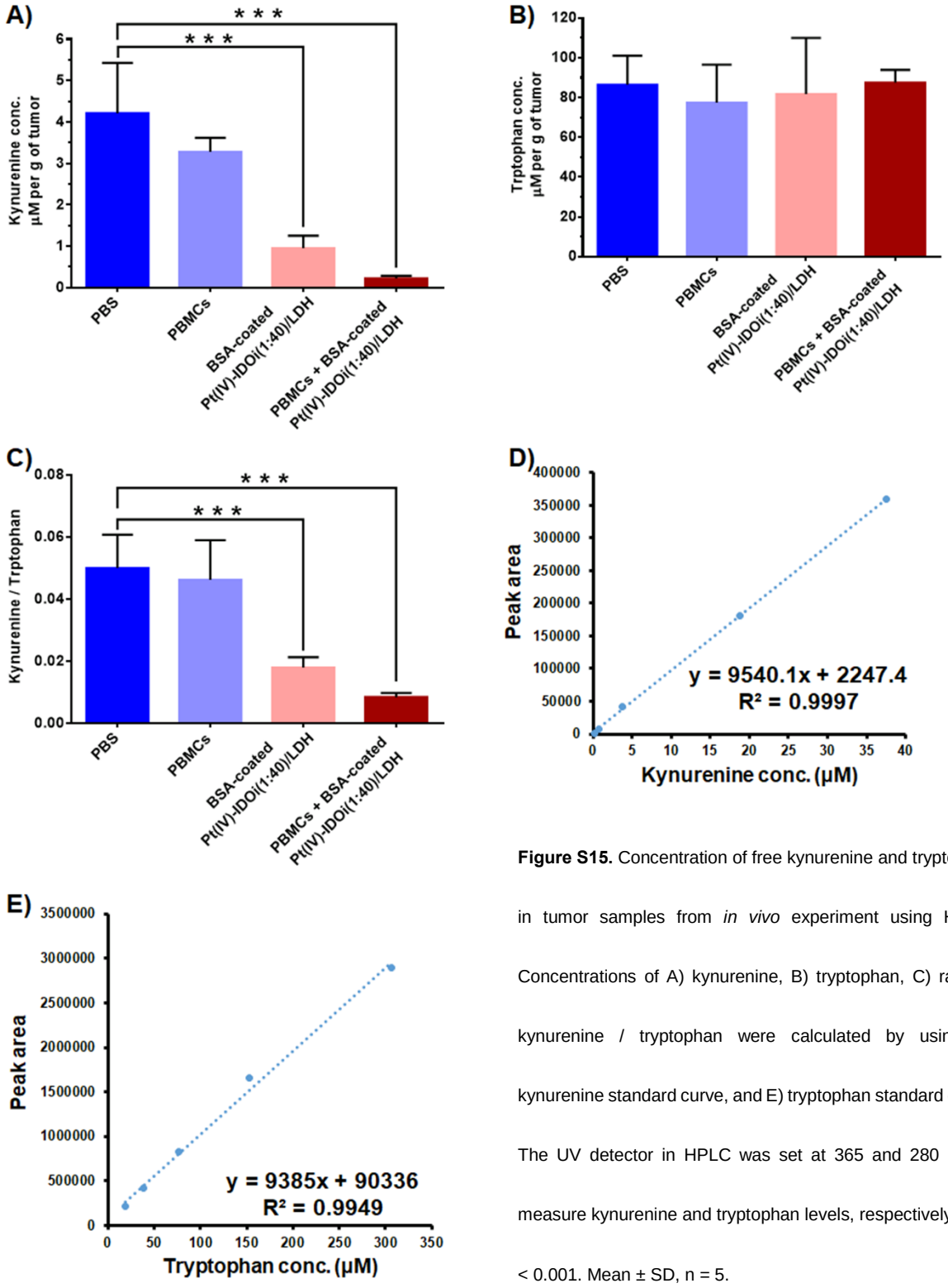

Figure S15. Concentration of free kynurenine and tryptophan in tumor samples from *in vivo* experiment using HPLC. Concentrations of A) kynurenine, B) tryptophan, C) ratio of kynurenine / tryptophan were calculated by using D) kynurenine standard curve, and E) tryptophan standard curve. The UV detector in HPLC was set at 365 and 280 nm to measure kynurenine and tryptophan levels, respectively. *** $p < 0.001$. Mean ± SD, n = 5.

Table S1. Measured co-loading nanoparticles containing Pt(IV) and/or IDOi.

Pt:IDOi	Loaded Pt (μmol/mg)	Loaded inhibitor (μmol/mg)
-	0.15	0
-	0	14.56
10:1	0.25	0.03
1:2	0.27	0.58
1:10	0.21	1.76
1:40	0.29	12.04
1:245	0.06	14.21

Table S2. Diameter and zeta potential of nanoplatform containing Pt(IV) and/or IDOi.

Sample	Number hydrodynamic size (d. nm)	Zeta potential (mV)
LDH	73.8 ± 2.1	46.0 ± 8.9
Pt(IV)/LDH	84.1 ± 10.1	41.6 ± 9.7
IDOi/LDH	182.6 ± 5.1	28.4 ± 3.9
Pt(IV)-IDOi(10:1)/LDH	117.2 ± 5.1	43.9 ± 11.1
Pt(IV)-IDOi(1:2)/LDH	158.2 ± 18.9	41.6 ± 8.9
Pt(IV)-IDOi(1:10)/LDH	176.9 ± 11.6	29.4 ± 5.4
Pt(IV)-IDOi(1:40)/LDH	216.7 ± 30.8	25.1 ± 9.6

Table S3. EC_{50} of different complexes in inhibiting the produce of kynurenine in HeLa cells. Cells were incubated with complexes and hIFN-γ for 48 h.

Complex	EC_{50}/μM
D-1MT	> 1000
IDOi	163 ± 24
IDO/LDH	4.0 ± 0.3
Pt(IV)-IDOi(1:40)/LDH	1.9 ± 0.2
Cisplatin + IDOi (1:40)	27.8 ± 0.1

Table S4. Diameter and zeta potential of nanoplatform containing Pt(IV) and/or IDOi after incubation with blood plasma at 0 h and 24 h (37 ºC).

Sample	Number hydrodynamic size (d. nm)		Zeta potential (mV)	
	0 h	**24 h (37 ºC)**	**0 h**	**24 h (37 ºC)**
LDH	357.0 ± 72.2	355.3 ± 23.0	-9.1 ± 5.1	-26.8 ± 1.7
Pt(IV)/LDH	503.2 ± 18.6	516.1 ± 47.9	-2.2 ± 2.2	-24.3 ± 1.6
IDOi/LDH	496.3 ± 59.5	497.0 ± 48.4	-32.4 ± 4.7	-23.4 ± 6.9
Pt(IV)-IDOi(1:40)/LDH	515.2 ± 55.7	547.4 ± 36.5	-24.2 ± 7.8	-25.0 ± 5.1

Table S5. Diameter and zeta potential of BSA-coated Pt(IV)-IDOi(1:40)/LDH with/without incubation with blood plasma at 37 ºC.

Sample	Number hydrodynamic size (d. nm)	Zeta potential (mV)
BSA-coated Pt(IV)-IDOi(1:40)/LDH	261.2 ± 49.8	-0.196 ± 0.1
BSA-coated Pt(IV)-IDOi(1:40)/LDH in blood plasma at 0 h	293.4 ± 18.3	-2.26 ± 0.6
BSA-coated Pt(IV)-IDOi(1:40)/LDH in blood plasma at 24 h	324.8 ± 64.7	-3.1 ± 0.4

References

[1] M.-F. Cheng, M.-S. Hung, J.-S. Song, S.-Y. Lin, F.-Y. Liao, M.-H. Wu, W. Hsiao, C.-L. Hsieh, J.-S. Wu, Y.-S. Chao, C. Shih, S.-Y. Wu, S.-H. Ueng, *Bioorg. Med. Chem. Lett.* **2014**, *24*, 3403-3406.

[2] Z. P. Xu, G. S. Stevenson, C.-Q. Lu, G. Q. Lu, P. F. Bartlett, P. P. Gray, *J. Am. Chem. Soc.* **2006**, *128*, 36-37.

[3] a) Z. Wang, R. Ma, L. Yan, X. Chen, G. Zhu, *Chem. Commun.* **2015**, *51*, 11587-11590; b) R. Ma, Y. Wang, L. Yan, L. Ma, Z. Wang, H. C. Chan, S. K. Chiu, X. Chen, G. Zhu, *Chem. Commun.* **2015**, *51*, 7859-7862.

[4] R. Ma, Z. Wang, L. Yan, X. Chen, G. Zhu, *J. Mater. Chem. B* **2014**, *2*, 4868-4875.

[5] Z. Gu, H. Zuo, L. Li, A. Wu, Z. P. Xu, *J. Mater. Chem. B* **2015**, *3*, 3331-3339.

[6] N. M. Silva, C. V. Rodrigues, M. M. Santoro, L. F. L. Reis, J. I. Alvarez-Leite, R. T. Gazzinelli, *Infect. Immun.* **2002**, *70*, 859-868.

[7] N. Anikeeva, D. Grosso, N. Flomenberg, Y. Sykulev, *Nat. Commun.* **2016**, *7*, 13264.